

## Prognostic Value of Tumor Architecture, Tumor-Associated Vascular Characteristics, and Expression of Angiogenic Molecules in Pancreatic Endocrine Tumors

Yu Takahashi,<sup>1,3</sup> Yuri Akishima-Fukasawa,<sup>1</sup> Noritoshi Kobayashi,<sup>1</sup> Tsuyoshi Sano,<sup>2</sup> Tomoo Kosuge,<sup>2</sup> Yuji Nimura,<sup>3</sup> Yae Kanai,<sup>1</sup> and Nobuyoshi Hiraoka<sup>1</sup>

**Abstract Purpose:** It is difficult to predict the biological behavior of pancreatic endocrine tumors (PETs). Our aim was to evaluate the prognostic significance of certain variables in PETs.  
**Experimental Design:** The following variables were examined in 37 patients with PETs and then compared with other clinicopathologic characteristics: histologic tumor structure; microvessel density (MVD) measured by three different methods, including a unique method involving calculation of solid area MVD; endothelial proliferation; and the immunohistochemical expression of vascular endothelial growth factor-A and CXC chemokine CXCL-12. Intratumoral vascular structures were analyzed by double immunofluorescence using 30- $\mu$ m-thick sections.  
**Results:** The presence of focal and intensive solid growth of tumor cells (large solid nests;  $P = 0.003$ ), low solid area MVD ( $P = 0.002$ ), a high endothelial cell proliferation index (EPI;  $P = 0.005$ ), and high expression of CXCL-12 in PET cells ( $P = 0.018$ ) were significant unfavorable prognostic indicators. The predominant structure of the overall tumor histology and the expression of vascular endothelial growth factor-A did not separate aggressive PETs. In areas of focal solid growth, tumor-associated blood vessels had obviously low MVD and high EPI, and their structures were poorly formed with highly abnormal features, in comparison with other areas. High expression of CXCL-12 in tumor cells was significantly associated with variables representing tumor growth, hematogenous tumor spread, low MVD, high EPI, and the presence of large solid nests.  
**Conclusions:** This study has provided novel findings on the prognostic features of tumor architecture and tumor-associated angiogenesis in PETs. CXCL-12 is the first candidate molecule in association with neoangiogenesis in PETs.

Pancreatic endocrine tumors (PETs) are uncommon neoplasms, and their prognostication is difficult when based purely on the histologic architecture and cytologic features of the tumor. Only the presence of distant metastases and local invasion to surrounding organs is the definitive criterion of malignancy (1–3). During the last few decades, various prognostic variables representing the proliferative or invasive

ability of tumor cells have been reported, such as tumor size, mitotic rate, Ki-67 proliferative index, and presence of vascular and perineural invasion (1–5). Other molecules have also been reported to be prognostic variables, such as cytokeratin 19 and CD99 (6, 7). The last WHO classification of PETs used some of these variables, in addition to conventional histopathologic tumor typing (1). However, this is still not enough for predicting the biological behavior of PETs because retrospective studies have shown that patients with PETs classified as “well-differentiated endocrine tumors,” “benign tumors,” or “tumors of uncertain behavior” sometimes suffer tumor recurrence or die of the disease (4, 6). To identify more reliable prognostic variables representing the biological characteristics of PETs, we analyzed their histologic structure, focusing especially on the solidness of the tumor growth pattern and attempted to classify them on this basis. At the same time, we examined the characteristics of intratumoral (i.t.) blood vessels, as these are closely associated with tumor architecture. In our experience, microvessel density (MVD) is lower in areas where tumor cells of PETs grow in a more solid pattern.

Normal endocrine tissues, including pancreatic islets of Langerhans and endocrine tumors, are characterized by high vascular density. In a murine pancreatic endocrine carcinoma model, RIP1-Tag2 transgenic mice expressing the SV40 T antigen in insulin-producing  $\beta$  cells, the tumor vasculature increases, and

**Authors' Affiliations:** <sup>1</sup>Pathology Division, National Cancer Center Research Institute; <sup>2</sup>Division of Hepatobiliary and Pancreatic Surgery, National Cancer Center Hospital, Tokyo, Japan; and <sup>3</sup>Division of Surgical Oncology, Department of Surgery, Nagoya University Graduate School of Medicine, Nagoya, Japan  
Received 6/12/06; revised 10/5/06; accepted 10/18/06.

**Grant support:** Ministry of Health, Labor, and Welfare of Japan grant-in-aid for Third-Term Comprehensive 10-Year Strategy for Cancer Control and Ministry of Education, Culture, Sports, Science, and Technology of Japan grant-in-aid for Scientific Research.

The costs of publication of this article were defrayed in part by the payment of page charges. This article must therefore be hereby marked *advertisement* in accordance with 18 U.S.C. Section 1734 solely to indicate this fact.

**Note:** Supplementary data for this article are available at Clinical Cancer Research Online (<http://clincancerres.aacrjournals.org/>).

**Requests for reprints:** Nobuyoshi Hiraoka, Pathology Division, National Cancer Center Research Institute, 5-1-1 Tsukiji, Chuo-ku, Tokyo 104-0045, Japan. Phone: 81-3-3542-2511; Fax: 81-3-3248-2463; E-mail: nhiraoka@gan2.res.ncc.go.jp.

© 2007 American Association for Cancer Research.  
doi:10.1158/1078-0432.CCR-06-1408

vascular morphology become abnormal during multistep carcinogenesis (8, 9). Tumor-associated blood vessels in various human cancers are structurally and functionally abnormal, showing increased permeability, delayed maturation, and potential for rapid proliferation (10, 11). The vessel defects may also facilitate hematogenous spread of tumor cells (12). Angiogenesis is essential for tumor growth and also plays an important role in hematogenous spread (13, 14). Measurement of MVD using immunohistochemistry is a widely used method for measuring angiogenic activity. Numerous studies have shown that elevated MVD is a significant predictive indicator of poor survival (13, 15). In human PETs, however, some recent studies have shown that low MVD is an unfavorable prognostic factor (16, 17), whereas others have suggested that MVD is not a predictive indicator of survival (18, 19). Thus, the relationship between MVD and biological behavior in human PETs is still controversial, although high MVD does not seem to be an unfavorable prognostic factor. It has been shown that angiogenic factors in many kinds of human cancers are related to metastatic dissemination, tumor aggressiveness, and short patient survival (20–22). Only vascular endothelial growth factor-A (VEGF-A) has been studied in human PETs, although there is still no evidence that it contributes to malignancy or patient survival (16–18). No attempt has been made to assess the prognostic value of angiogenic factors other than VEGF-A in PETs.

The aim of the present study was to investigate histologic tumor architecture, tumor-associated angiogenesis, and expression of angiogenic molecules in a series of resected PETs and to evaluate the potential prognostic significance of these variables.

### Materials and Methods

**Patients and samples.** This study was approved by the Ethics Committee of the National Cancer Center, Tokyo, Japan. Clinical and pathologic data and the specimens used for immunohistochemical analysis were obtained through a detailed retrospective review of the medical records of all 37 Japanese patients with PETs who had undergone initial surgical resection between 1981 and 2004 at the National Cancer Center Central Hospital, Japan. The median age of the patients at surgery was 55 years (range, 18–81 years; mean, 52.9 years). None of the patients

had received prior therapy and underwent potentially curative resection: pancreatoduodenectomy in 19 cases, distal pancreatectomy in 12 cases, tumor enucleation in 4 cases, and total pancreatectomy in 2 cases. Tumors were classified according to the WHO classification (1) into the following groups: benign well-differentiated endocrine tumors (referred to as WHO-1 in this report), well-differentiated endocrine tumors of uncertain behavior (WHO-2), well-differentiated endocrine carcinoma (WHO-3), and poorly differentiated endocrine carcinoma (WHO-4). Follow-up was available in all cases and ranged from 2 to 275 months (median, 46.8 months; mean, 65.2 months). During the follow-up period, nine patients presented with evidence of disease progression as liver metastasis, and two of them presented with evidence of local recurrence. The latest survival data were collected on December 31, 2004. The total survival rate was 78% at 5 years and 65% at 10 years. The clinicopathologic features of the patients are summarized in Table 1. Eight variables (large tumor size, presence of invasion to surrounding organs, presence of lymph node metastasis, presence of hematogenous metastasis, presence of vascular invasion, presence of perineural invasion, absence of functional hormone syndrome, and high Ki-67 index) had been reported to be unfavorable prognostic factors (1, 2). In our series, all these variables except “absence of functional hormone syndrome” were closely correlated with short survival (Table S1).

For histopathologic examinations, all tissue specimen was cut to make sections. Four-micrometer formalin-fixed, paraffin-embedded sections were prepared and stained with H&E. Vascular invasion was assessed by histopathologic examination, using H&E-stained tissue sections and sections stained for elastic fibers with Maeda’s resorcin/fuchsin solution (Muto Pure Chemicals, Tokyo, Japan). With regard to the structural pattern of tumor histology, tumors were divided into four groups by the following criteria based on predominant architecture (Fig. 1A–D): grade 1, tumors consisting of small nests (with 1–5 tumor cells in the minor axis); grade 2, tumors consisting of moderate nests (with 6–10 tumor cells in the minor axis); grade 3, tumors consisting of large solid nests (with ≥11 tumor cells in the minor axis); and grade 4, tumors showing a diffuse growth pattern. The ratio of each solid grade was determined each tumor area in middle-power view and was calculated for the entire tumor area. Then the predominant grades were determined for each PET. PET with large solid nests was defined if there was at least a large solid nest in the tumor, regardless of the overall solid grading. Grading was carried out by two observers independently.

**Immunohistochemistry.** Immunohistochemistry was done on the formalin-fixed, paraffin-embedded tissue sections using the avidin-biotin complex method as described previously (23). We used 4-μm-thick sections of representative blocks with antibodies against the

**Table 1.** Summary of patients’ demographics

Variables	WHO-1 (n = 6)	WHO-2 (n = 14)	WHO-3 (n = 15)	WHO-4 (n = 2)	Total
Sex (male/female)	2/4	6/8	6/9	1/1	15/22
Median age (y)	58.5	55.5	52	30	55
Functional hormone syndrome*	0	2	2	0	4
Mean tumor size (cm)	1.2	3.6	6.4	10.0	4.7
Invasion to surrounding organs	0	0	10	2	12
Lymph node metastasis	0	0	13	2	15
Hematogenous metastasis†	0	1	8	1	10
Vascular invasion	0	4	13	2	19
Perineural invasion	0	3	10	2	15
Ki-67 labeling index >5	0	4	10	2	16
Follow-up					
Alive and well without disease	5	13	7	1	26
Alive with disease	0	0	3	0	3
Dead of disease	0	1	4	1	6
Dead of other cause	1	0	1	0	2

\*Four patients showed the clinical manifestation associated with hypersecretion of insulin in two cases: glucagon in one and gastrin in another.

†Tumor metastasized to liver or other organs by hematogenous spreading before and/or after the surgical resection of PETs.

following: chromogranin A (poly; 1:500), synaptophysin (poly; 1:50), neuron-specific enolase (BBS/NC/VI-H14; 1:100), CD31 (JC/70A; 1:50), CD34 (QEnd 10; 1:100), Factor VIII (poly; 1:1000),  $\alpha$ -smooth muscle actin ( $\alpha$ -SMA; 1A4; 1:50), and Ki-67 (MIB-1; 1:100) from DAKO (Glostrup, Denmark); CD56 (NCC-Lu-243; 1:50) from Nippon Kayaku (Tokyo, Japan); VEGF-A (poly; 1:100) from Santa Cruz Biotechnology (Santa Cruz, CA); and CXCL-12 (79018; 1:50) from R&D Systems, Inc. (Minneapolis, MN). As a brief description, the sections were deparaffinized and rehydrated. After blocking of endogenous peroxidase with methanol containing 0.3% H<sub>2</sub>O<sub>2</sub>, the sections were autoclaved at 121 °C for 10 min in citrate buffer (10 mmol/L sodium citrate, pH 6) for antigen retrieval. After blocking with normal goat serum, the sections were reacted overnight with appropriately diluted primary antibodies. The sections were then reacted sequentially with biotin-conjugated anti-mouse immunoglobulin G antibodies (Vector Laboratories, Burlingame, CA) and Vectastain Elite ABC reagent (Vector Laboratories). For staining VEGF-A, the sections were boiled at 95 °C for 10 min for antigen retrieval. Diaminobenzidine was used as the chromogen, and the nuclei were counterstained with hematoxylin. For semiquantitative assessments of the immunohistochemical results for VEGF-A and CXCL-12, cytoplasmic staining intensity and the proportion of positive tumor cells were recorded. A staining index (with a value of 0-9) was calculated as the product of staining intensity (0-3) and area of positive staining (0, <1%; 1, 1-10%; 2, 10-50%; 3, >50%; ref. 23). The upper quartile was used as the cutoff point. The Ki-67 labeling index was determined as described previously (23). Immunohistochemical double staining for CD34 and Ki-67 was also done as described previously (24). Initially, Ki-67 was stained and visualized with diaminobenzidine as a brown-colored chromogen, followed by detachment of antibodies; then secondary immunohistochemistry was done to detect CD34; and the reaction product was visualized with VIP as a purple-colored chromogen (Vector Laboratories).

**Evaluation of i.t. MVD.** For evaluation of i.t. MVD, microvessels were detected by morphologic observation and immunohistochemical labeling with the endothelial markers CD31, CD34, and Factor VIII. In our preliminary study, three different markers detected endothelial cells similarly. CD34 showed the strongest intensity among them and could detect endothelial cells easily, but sometimes, it labeled fibroblasts that could be easily distinguished from vascular endothelial cells by their histology. Factor VIII showed the weakest staining intensity among them. Then we used CD34 for MVD assay and CD31 for immunofluorescence double staining. All independent CD34-positive vessel structures were counted, irrespective of the presence of an identifiable lumen. For assessment of MVD, we used three different methods as follows. Average MVD (Av-MVD) was analyzed by selecting 10 randomized fields per tumor at a magnification of  $\times 200$  (0.95 mm<sup>2</sup> per field), and the number of CD34-positive vessel structures in each field was counted. The mean number of vessels was then calculated after exclusion of the lowest and highest values measured (16). Hotspot MVD was assessed by a modification of the Weidner technique (21). The H&E-stained tissue sections were screened, and three areas with the most intense vascularization were selected at low magnification. We then counted CD34-positive vessels at a magnification of  $\times 200$ , and the average counts for the three fields were calculated. For solid area MVD (S-MVD), the H&E-stained tissue sections were screened, and we selected three areas showing the most solid growth pattern of tumor cells, which often contained large solid nests or a diffuse growth pattern. Then CD34-positive vessels at a magnification of  $\times 200$  were counted in each corresponding area. The average counts of the three fields was calculated and defined as the S-MVD. Two observers, having no access to the patient data, evaluated independently MVD, morphological vessel characters, and proliferating endothelial cells described below. Their final value was the average of the value counted by the two observers. To assess intraobserver reproducibility, several tissue sections were counted thrice by each observer. To assess interobserver reproducibility, 10 data counted by each observer for the same tumor were compared (16).

**Immunofluorescence double staining.** Immunofluorescence double staining was done on 30- $\mu$ m-thick, formalin-fixed, paraffin-embedded tissue sections as described previously (24), with some modifications. All antibodies were diluted in 0.2% Triton X-100 and 5% skim milk in TBS-T.  $\alpha$ -SMA antigens were stained by the CSA system (DAKO) with our modification, and then CD31 was stained with CSAII (DAKO). Reaction time for the primary and secondary antibodies was extended to overnight and 1 h, respectively. After reaction with biotin-conjugated tyramide solution, the sections were incubated with Texas Red-conjugated avidin (1:200) for 1 h at room temperature. After detaching the antibodies by acid treatment (100 mmol/L glycine/HCl, pH 2.2) for 2 h, the sections were stained with CD31 using CSAII according to the manufacturer's instructions with modifications. Just after reaction of the sections with FITC-conjugated tyramide, the sections were washed and mounted with Vectashield mounting medium (Vector Laboratories). Immunostained tissue sections were analyzed with a confocal microscope (LSM5 Pascal; Carl Zeiss Jena GmbH, Jena, Germany) equipped with a 15-mW Kr/Ar laser. The confocal files were saved, compiled, and fused to make three-dimensional pictures.

To estimate the branching frequency of blood vessels, 12 randomized fields were selected for each tumor at a magnification of  $\times 200$ . The distance of blood vessels between the closest two branches in each field was measured, and the mean length for each tumor was calculated, which we termed the unbranched vessel length. To estimate variability in the luminal diameter of blood vessels, 12 randomized fields were selected for each tumor at a magnification of  $\times 400$ . The maximum and minimum luminal diameters of blood vessels between the closest two branches in each field were measured, and the average of the difference in diameter was calculated. To evaluate abnormality of blood vessels showing irregular vessel wall shapes and distortion, i.t. vessels were divided into five categories: category 1 corresponded to regular vessels in normal islets of Langerhans, category 5 corresponded to the most severely changed vessels as shown in Fig. 4G to I, and categories 2 to 4 corresponded to vessels with mild to severe abnormalities between categories 1 and 5.

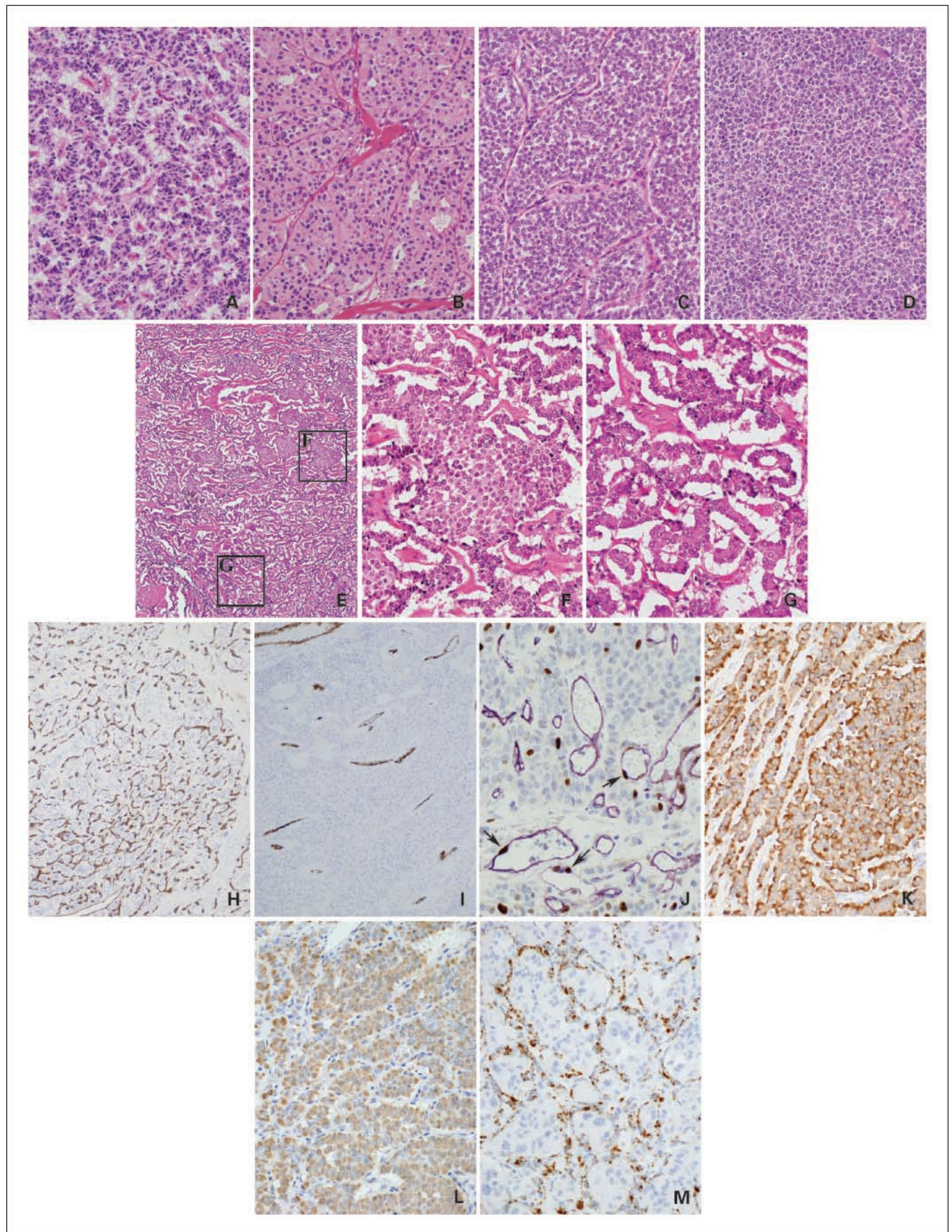
**Endothelial cell proliferation in i.t. blood vessels.** To evaluate the proliferation of endothelial cells, tumor tissues that had been double stained for Ki-67 and CD34 were assessed by modified previous methods (25, 26). Fifty randomized fields at a high magnification ( $\times 400$ ) were selected for each tumor, and we counted the number of CD34-expressing endothelial cells with Ki-67-positive nuclei in each field, then the total amount was defined as the endothelial cell proliferation (ECP). The ECP proliferation index (EPI) was defined as the ECP divided by the Av-MVD that was assessed in the same fields because MVD was different in each tumor.

**Statistical analysis.** Statistical analyses were done with StatView-J 5.0 software (Abacus Concepts, Berkeley, CA) and SPSS statistical software version 12.0 (SPSS, Inc., Chicago, IL). Association between categorical variables was examined by Fisher's exact probability test. Mann-Whitney nonparametric tests were used to compare categorical with continuous tumor variables when there were two categories, whereas Kruskal-Wallis nonparametric tests were used instead when there were more than two categories. Differences at  $P < 0.05$  were considered significant. Survival rates were computed by the Kaplan-Meier method and compared by the log-rank test.

## Results

The clinicopathologic characteristics of the 37 patients with PETs are described in Materials and Methods and Table 1.

**Histologic structural pattern.** The histologic pattern of tumor growth was studied to clarify whether it could predict tumor behavior. Initially, we classified PETs into four categories based on the solidness of the predominant tumor histology, ranging from grade 1, which was least solid, to grade 4, which showed



Downloaded from <http://aacrjournals.org/clinccancerres/article-pdf/13/1/187/1968474/187.pdf> by guest on 13 June 2024

the most solid and diffuse growth (Fig. 1A-D). Most of the PETs were classified as grade 1 (19 of 37; Table 2), which included tumors with a predominant histologic structure showing a thin trabecular, gyriform, or pseudoglandular pattern. All of the grade 3 PETs belonged to WHO-3, and grade 4 PETs belonged to WHO-4. There was no significant correlation between any of the grades and disease-free survival, but disease-free survival became closely correlated when grade 1 and 2 PETs were combined (Fig. 2A).

We then selected PETs that had a "large solid nest" defined as the presence of  $\geq 11$  tumor cells in the minor axis, independent of the overall tumor histologic pattern (Fig. 1E-G). Twenty PETs had large solid nests, including five grade 1 PETs, seven grade 2 PETs, and eight grade 3 and grade 4 PETs (Table 2). Interestingly, all the patients that suffered tumor recurrence had PETs with large solid nests, and all the patients without large solid nests remained disease-free. The presence of large solid nests was a significant factor correlated with disease-free survival (log-rank test,  $P = 0.003$ ; Fig. 2B). The presence of large solid nests was significantly correlated with tumor size ( $P = 0.008$ ), invasion to surrounding organs ( $P = 0.002$ ), lymph node metastasis ( $P = 0.018$ ), hematogenous metastasis ( $P = 0.0006$ ), vascular invasion ( $P = 0.0002$ ), and Ki-67 index ( $P = 0.007$ ; Table S1).

**MVD.** The relationship between MVD and biological behavior in human PETs is controversial (16–18), probably as a result of how MVD is counted. To clarify whether MVD is related to tumor behavior and to select the best way to count MVD, we tried to measure MVD of PETs using three different counting methods (Materials and Methods; Fig. 1H and I): Av-MVD, hotspot MVD, and S-MVD. Av-MVD ranged from 59.4 to 423.5 vessels per field (mean, 189.1; median, 167.6); hotspot MVD ranged from 132.3 to 625.0 vessels per field (mean, 288.3; median, 268.0); and S-MVD ranged from 30.0 to 468.3 vessels per field (mean, 161.5; median, 132.3). Av-MVD and S-MVD decreased according to the progression of PETs by the WHO classification, and this was statistically significant (Kruskal-Wallis test: Av-MVD,  $P = 0.010$ ; S-MVD,  $P = 0.003$ ; Fig. 3A and Fig. S1). Hotspot MVD did not show apparent differences among the WHO classes ( $P = 0.500$ ; Fig. S1). When all the PETs were divided into two groups based on median MVD, the high MVD group showed longer patient survival than the low MVD group (Fig. 3B and Fig. S1). The difference was clearer for S-MVD (log-rank test,  $P = 0.002$ ), and the high S-MVD group included no patients with recurrent tumors. S-MVD was significantly correlated with tumor size ( $P = 0.002$ ), invasion to surrounding organs ( $P = 0.001$ ), lymph node metastasis ( $P = 0.0006$ ), hematogenous metastasis ( $P = 0.0004$ ), vascular invasion ( $P < 0.0001$ ), perineural invasion ( $P = 0.007$ ), and Ki-67 index ( $P = 0.0002$ ; Table S1).

**Vascular ECP.** The dynamics of neoangiogenesis in PETs was assessed by ECP (Materials and Methods; Fig. 1J). ECP ranged from 0 to 26 (mean, 7.59; median, 7). Surprisingly, the ECP was higher in low S-MVD tumors ( $P = 0.011$ ; Fig. 3C). EPI (Materials and Methods; range, 0.00–0.27; mean, 0.057;

**Table 2.** Relationship between histologic structural grades or tumors with large solid nests and WHO classification of pancreatic endocrine tumors

	Grade 1	Grade 2	Grade 3	Grade 4	Total cases
WHO-1	4 (1)	2 (2)	0	0	6 (3)
WHO-2	11 (2)*	3 (1)	0	0	14 (3)
WHO-3	4 (2)**	5 (4)*	6 (6)****	0	15 (12)
WHO-4	0	0	0	2 (2)*	2 (2)
Total	19 (5)	10 (7)	6 (6)	2 (2)	37 (20)

NOTE: The numbers of patients with PET having large solid nests are in parentheses.

\*n, number of asterisks (\*) represent numbers of patients with PET recurrence.

median, 0.038) was also higher in PETs with low S-MVD and was significantly correlated with WHO classification (Kruskal-Wallis test,  $P = 0.001$ ; Fig. 3D). When patients were divided into two groups by the median EPI, the high EPI group showed significantly shorter disease-free survival than the low EPI group (log-rank test,  $P = 0.005$ ; Fig. 3E). EPI was significantly correlated with tumor size ( $P < 0.0001$ ), invasion to surrounding organs ( $P = 0.005$ ), lymph node metastasis ( $P = 0.020$ ), hematogenous metastasis ( $P = 0.003$ ), vascular invasion ( $P < 0.0001$ ), and Ki-67 index ( $P = 0.0008$ ; Table S1).

**Vascular characteristics.** We then analyzed the structures of blood vessels to determine whether blood vessels change to poorly formed vessels with multiple abnormalities, in association with tumor progression. We analyzed 9 PETs with high S-MVD and 13 PETs with low S-MVD that were available for immunofluorescence analysis using 30- $\mu$ m-thick tissue sections stained for CD31 and  $\alpha$ -SMA. There were fine mesh-like structures consisting of smooth, thin, and relatively regular vessels in tumors with high S-MVD (Figs. 1H and 4D-F). The rough structure of the vasculature in tumors with high S-MVD was similar to the vascular features of normal islets of Langerhans (Fig. 4A-C), although the vessels in the tumors were thick, and their detailed structures were irregular. In contrast, the vasculature in PETs with low S-MVD was less branched and relatively straight (Fig. 4J), consisting of thicker, more irregularly shaped and often distorted vessels (Figs. 1I, 4G-I and 4L). In high-power view, instead of mature branches, there were many very small and irregular buds on the vessels, which showed highly abnormal features (Fig. 4I).  $\alpha$ -SMA-positive cells covered these irregular buds. The luminal diameter of vessels was more variable in PETs with low S-MVD than in PETs with high S-MVD (Fig. 4K). Almost all the i.t. blood vessels were covered by  $\alpha$ -SMA-positive mural cells, although  $\alpha$ -SMA-positive multiple layers were often observed in PETs with low S-MVD. These findings indicated that i.t. blood vessels in PETs with low S-MVD were poorly formed blood vessels with multiple abnormalities,

**Fig. 1.** A to D, histologic structural grading of PETs based on the degree of solid growth of tumor cells in the predominant architecture. Grade 1 tumor consists of small nests (A). Grade 2 tumor consists of moderate nests (B). Grade 3 tumor consists of large solid nests (C). Grade 4 tumor grows in a diffuse solid pattern (D). E to G, large solid nests. Tumor cells proliferate predominantly in a trabecular pattern and sometimes form large solid nests focally in low-power view (E). Middle-power view of large solid nests (F) and trabecular pattern (G). H to M, immunohistochemistry. CD34-labeled endothelial cells are detected in PET with high MVD (H) and in PET with low MVD (I) in low-power view. J, CD34 (purple) is expressed in vascular endothelial cells, and nuclei of proliferating cells are labeled by Ki-67 (brown) in high-power view. Arrows, proliferating endothelial cells. K, VEGF-A stained in cytoplasm of PET cells in middle-power view. CXCL-12 stained in PET cells (L) and blood vessels (M) in middle-power view.

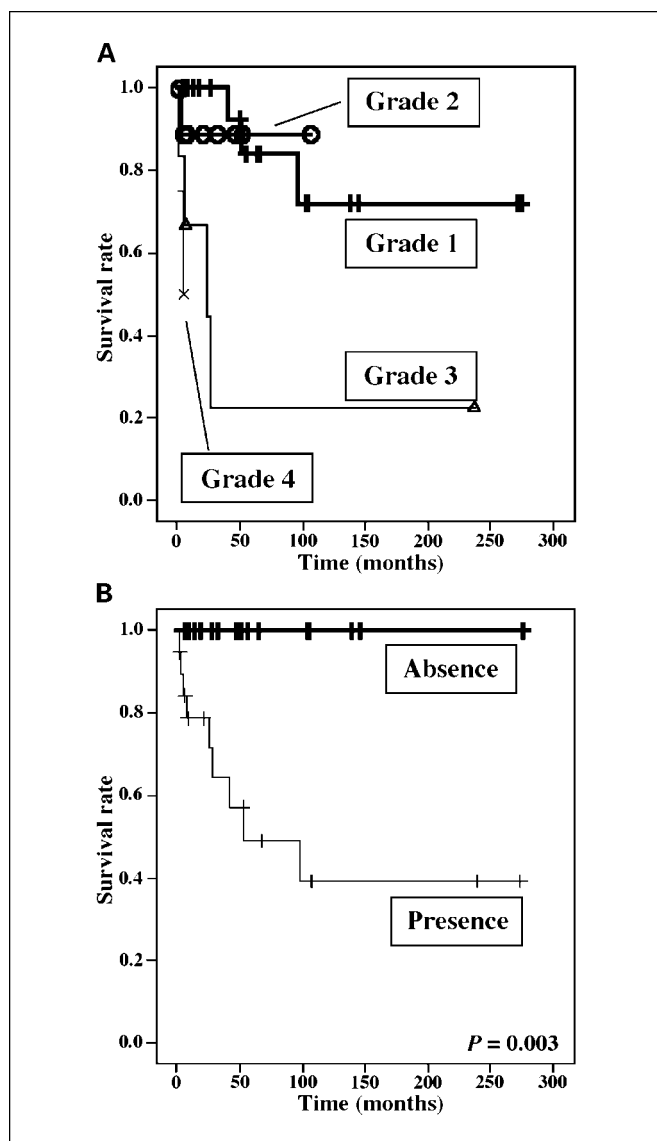


**Fig. 2.** Kaplan-Meier survival curves of the 37 patients with PETs. *A*, PETs are classified by predominant histological structures into four grades. There was no significant correlation between this classification and disease-free survival. *B*, PETs are divided by the presence or absence of large solid nests. Patients with PETs showing large solid nests had significantly shorter disease-free survival (log-rank test,  $P = 0.003$ ).

whereas blood vessels in PETs with high S-MVD still had the characteristics of endocrine organs.

**Expression of VEGF-A and CXCL-12 in PETs.** To assess the angiogenic factors in PETs, we analyzed the expression of VEGF-A and CXCL-12 in tumor cells and i.t. blood vessels by immunohistochemistry (Fig. 1K-M). CXCL-12 is known to be a CXC chemokine involved in the recruitment of circulating endothelial progenitor cells from bone marrow to the target organs (27, 28). High expression of CXCL-12 in tumor cells was significantly correlated with high EPI ( $P = 0.020$ ; Table 3) and low S-MVD ( $P = 0.0006$ ; Table 3), although expression of CXCL-12 in i.t. blood vessels and VEGF-A expressed in tumor cells did not closely correlate with EPI and S-MVD (Table 3). High expression of VEGF-A in tumor cells was significantly correlated with high expression of CXCL-12 in i.t. blood vessels

( $P < 0.0001$ ) but not to other clinicopathologic variables, including expression of CXCL-12 in tumor cells (Table 3). A high value of CXCL-12 in the tumor was significantly correlated with marked vascular invasion ( $P = 0.0006$ ), the presence of hematogenous metastasis ( $P = 0.006$ ), large tumor size ( $P = 0.035$ ), a high Ki-67 index ( $P = 0.006$ ), and the presence of large solid nests ( $P = 0.018$ ). Furthermore, PETs having high amounts of CXCL-12 in the tumor cells were closely correlated with a shorter disease-free patient survival rate (log-rank test,  $P = 0.018$ ; Fig. 3F).

## Discussion

In this study, we found a new histologic marker for predicting the biological behavior of PETs (i.e., "the presence of focal large solid nests"), which is independent of the predominant histologic structure. Then we measured S-MVD and showed a close correlation between low MVD and an unfavorable prognosis in PETs. Paradoxically, i.t. vessels of PETs with a high MVD showed low EPI and vice versa. Morphometric analysis showed that blood vessels in PETs with low MVD were more poorly formed and had more irregular and abnormal features, whereas blood vessels in PETs with high MVD showed relatively regular mesh-like features similar to vessels in normal islets of Langerhans. These findings imply that a high MVD seems to be a characteristic of blood vessels in islets of Langerhans, and that EPI can be a hallmark of angiogenic activity in tumor-associated blood vessels in PETs. Our data also suggest that EPI and S-MVD are predictors of the biological behavior of PETs. We analyzed angiogenic factors in PETs and found that high EPI and low MVD were significantly correlated with high expression of CXCL-12 in tumor cells but not with the expression of CXCL-12 in i.t. blood vessels and VEGF-A. Combined with the data for the relationship between CXCL-12 and other variables, it is suggested that CXCL-12 produced in tumor cells is involved in the angiogenesis of tumor-associated vessels and hematogenous spread as well as proliferation of tumor cells and thus may contribute to the aggressiveness of PETs. CXCL-12 is the first molecule to be highlighted as a possible angiogenic factor playing important roles in the neoangiogenesis of PETs. Thus, we have provided novel data on the prognostic features of tumor architecture and tumor-associated angiogenesis in PETs.

In contrast to the predominant histologic structures, the presence of focal large solid nests delineated PETs with aggressive behavior. Even in grade 1 and 2 PETs, patients with large solid nests had significantly shorter disease-free survival than patients without them ( $P = 0.024$ ). Interestingly, metastatic PETs showed almost the same histologic architecture as the original pancreatic tumors and were not occupied by tumor cells with solid growth. These findings suggest that tumor cells in large solid nests are not more progressed or more malignant than their origin, and that the presence of large solid nests represents the potential for tumor malignancy.

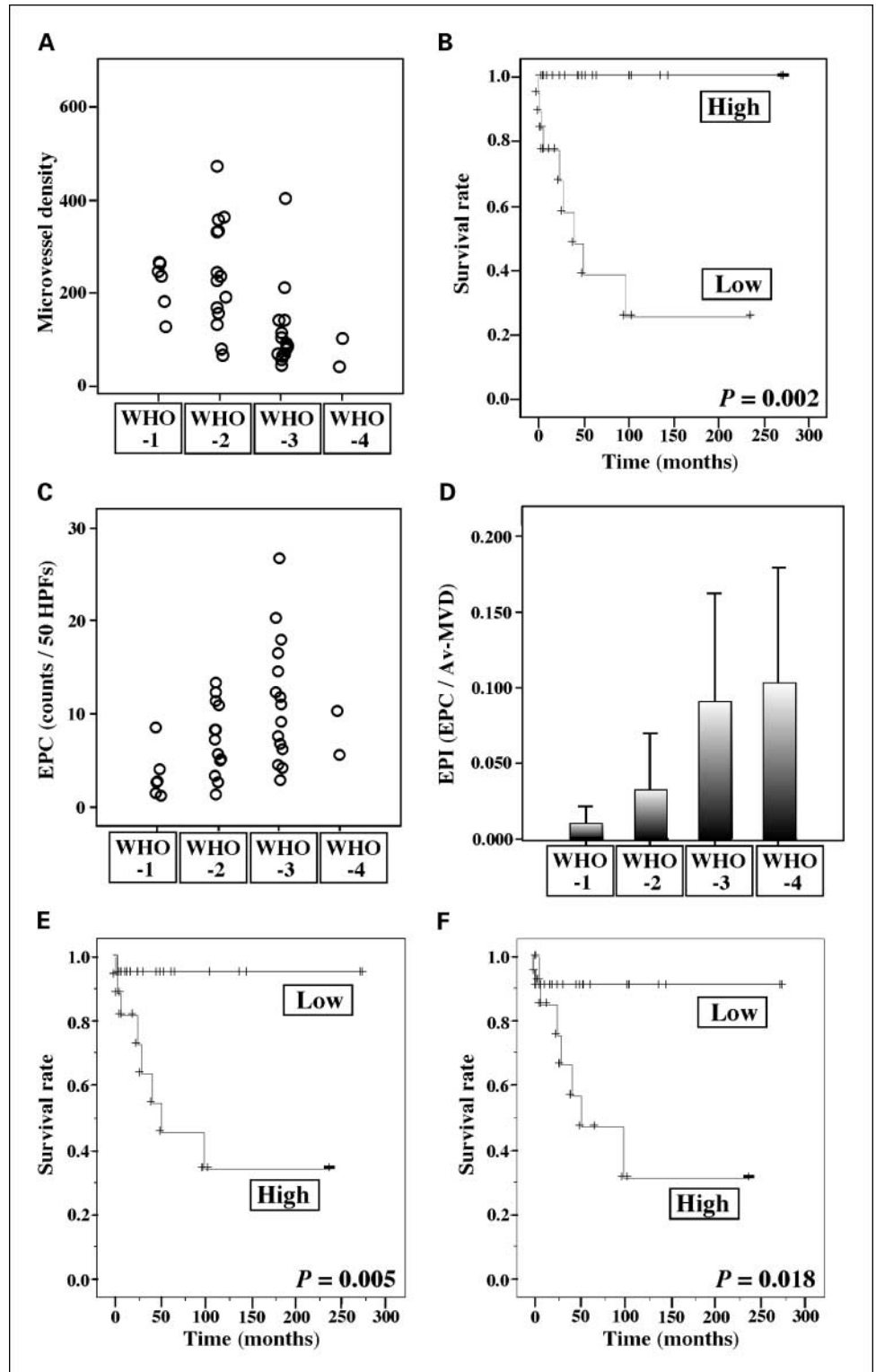
By comparing three methods for evaluation of MVD, we found that the best variable for predicting the representative biological characteristics of PETs was S-MVD. This seems reasonable because in PETs, we showed that a focal tumor structure showing the most solid growth represents the behavior of the tumor as a whole. Morphometric analysis also showed that irregularity and abnormality of i.t. blood vessels were associated with tumor growth pattern where the vessels were present. These findings

imply that tumor architecture is closely correlated with local vessel formation, and that tumor cells and blood vessels seem to be a pair of components within a single structure.

Our results indicate that EPI and MVD can be prognostic variables in patients with PETs. Abnormal tumor-associated blood vessels tend to grow rapidly (10), consistent with the fact that PETs with more poorly formed blood vessels have a high

EPI. EPI is also significantly correlated with hematogenous spread (vascular invasion,  $P < 0.0001$ ; hematogenous metastasis,  $P = 0.003$ ) and survival ( $P = 0.005$ ) in PETs. Recently, similar results were indicated in the other tumor by Stefansson et al. That is, increased vascular proliferation was associated with aggressive features of tumors and was an independent prognostic factor in endometrial carcinoma (26).

**Fig. 3.** A, C, and D, relationship between vascular index and WHO classification. B, E, and F, Kaplan-Meier survival curves of 37 patients with PETs. A, S-MVD significantly decreased according to progression of PETs in terms of the WHO classification (Kruskal-Wallis test,  $P = 0.003$ ). B, patients were divided into two groups by median S-MVD. The high S-MVD group showed significantly longer survival than the low S-MVD group (log-rank test,  $P = 0.002$ ). C, EPC significantly increased according to progression of PETs in terms of the WHO classification (Kruskal-Wallis test,  $P = 0.019$ ). D, EPI significantly increased according to progression of PETs in terms of the WHO classification (Kruskal-Wallis test,  $P = 0.001$ ). E, patients were divided into two groups by median EPI. The high EPI group showed significantly shorter survival than the low EPI group (log-rank test,  $P = 0.005$ ). F, patients were divided into two groups by the quartile value of CXCL-12 expressed in the tumor cells. Patients with PETs showing high expression of CXCL-12 in the tumor cells had significantly shorter survival than those whose tumors showed low expression (log-rank test,  $P = 0.018$ ).



Downloaded from <http://aacrjournals.org/clinccancerres/article-pdf/13/1/187/1968474/187.pdf> by guest on 13 June 2024

What kinds of molecules are involved in tumor-associated angiogenesis in PETs? It has been reported that in many kinds of cancers VEGF produced in tumor cells accelerates tumor-associated angiogenesis, leading to tumor growth and a high frequency of hematogenous tumor cell spread (14). VEGF-A expression in PETs is reported to be not closely correlated with MVD (16, 18) or to be closely correlated with high MVD (17). In our series, there was no close correlation of VEGF-A expression with growth of blood vessels, hematogenous spread, or tumor growth in PETs, but with high expression of CXCL-12 in i.t. blood vessels. CXCL-12 has chemotactic activity for leukocytes (28) and stem cells (29). Grunewald et al. reported that VEGF-A induces adult neovascularization mediated by CXCL-12 expression in the microenvironment. VEGF-A recruits endothelial progenitor cells from the bone marrow to the blood and induces expression of CXCL-12, which traps and correctly posi-

tions endothelial progenitor cells around growing vessels in tissues (27). Our study suggested that VEGF-A induced the expression of CXCL-12 in tumor vessels, although such events did not lead to tumor-associated neoangiogenesis in PETs. In contrast, high EPI was closely correlated with high CXCL-12 produced in tumor cells ( $P = 0.020$ ). High expression of CXCL-12 in tumor cells was also positively correlated with variables of hematogenous tumor spread (versus vascular invasion,  $P = 0.0006$ ; versus hematogenous metastasis,  $P = 0.006$ ) and tumor growth (versus tumor size,  $P = 0.035$ ; versus Ki-67 index,  $P = 0.006$ ) and also with shorter patient survival ( $P = 0.018$ ). These findings suggest that CXCL-12 produced in tumor cells is involved in the aggressive features of tumor mediated by neoangiogenesis and tumor growth. Orimo et al. reported that carcinoma-associated fibroblasts in breast cancer secrete CXCL-12, which promotes the growth of the tumor cells both directly

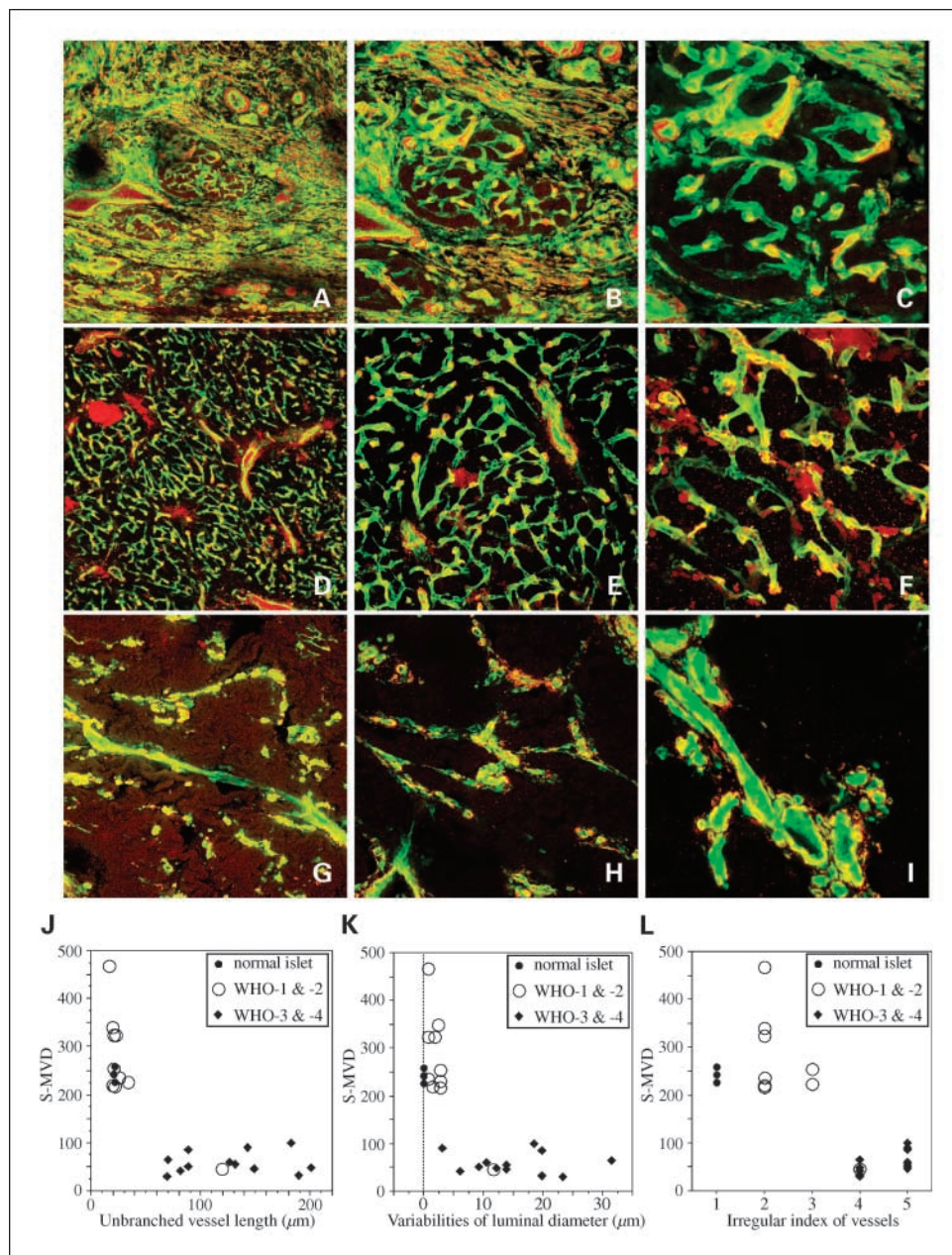


**Fig. 4.** Characterization of tumor-associated blood vessels in double immunofluorescence examination of CD31 (green) and  $\alpha$ -SMA (red) using 30- $\mu$ m-thick sections. Normal islet of Langerhans in low-power (A), middle-power (B), and high-power (C) view. PET with high S-MVD in low-power (D), middle-power (E), and high-power (F) view. PET with low S-MVD in low-power (G), middle-power (H), and high-power (I) view. J to L, morphometric analyses of PETs. I.t. blood vessels were examined for unbranched vessel length (J), variability of luminal diameter (K), and vessel irregularity (L).



**Table 3.** Relationship between clinicopathologic variables and VEGF-A or CXCL-12

Variables	n	VEGF-A			CXCL-12 in tumor cells			CXCL-12 in blood vessels		
		High (n = 19)	Low (n = 18)	P	High (n = 19)	Low (n = 18)	P	High (n = 19)	Low (n = 18)	P
Age (y)										
≤55	19	8	11	NS	8	11	NS	8	11	NS
>55	18	10	8		7	11		11	7	
Sex										
Female	22	13	9	NS	10	12	NS	13	9	NS
Male	15	5	10		5	10		6	9	
Functional hormone syndrome										
Absence	33	16	17	NS	14	19	NS	17	16	NS
Presence	4	2	2		1	3		2	2	
Tumor size (cm)										
<2	13	3	10	0.038	2	11	0.035	4	9	NS
≥2	24	15	9		13	11		15	9	
Invasion to surrounding organs										
Absence	25	12	13	NS	7	18	NS	15	10	NS
Presence	12	6	6		8	4		4	8	
Lymph node metastasis										
Absence	22	8	14	NS	6	16	NS	11	11	NS
Presence	15	10	5		9	6		8	7	
Hematogenous metastasis*										
Absence	27	12	15	NS	7	20	0.006	13	14	NS
Presence	10	6	4		8	2		6	4	
Vascular invasion										
Absence	18	6	12	NS	2	16	0.0006	9	9	NS
Presence	19	12	7		13	6		10	9	
Perineural invasion										
Absence	22	10	12	NS	7	15	NS	12	10	NS
Presence	15	8	7		8	7		7	8	
Ki-67 labeling index										
≤5	21	8	13	NS	4	17	0.006	9	12	NS
>5	16	10	6		11	5		10	6	
Histologic structural grades										
1 + 2	29	15	14	NS	10	19	NS	18	11	0.019
3 + 4	8	3	5		5	3		1	7	
Large solid nests										
Absence	17	7	10	NS	3	14	0.018	9	8	NS
Presence	20	11	9		12	8		10	10	
S-MVD										
High	18	7	11	NS	2	16	0.0006	10	8	NS
Low	19	11	8		13	6		9	10	
EPI										
High	18	11	7	NS	11	7	0.020	10	8	NS
Low	19	7	12		4	15		9	10	
VEGF-A										
High	18				10	8	NS	16	2	<0.0001
Low	19				5	14		3	16	
CXCL-12 in tumor cells										
High	15	10	5	NS				8	7	NS
Low	22	8	14					11	11	
CXCL-12 in vessels										
High	19	16	3	<0.0001	8	11	NS			
Low	18	2	16		7	11				

Abbreviation: NS, not significant.

\*Tumor metastasized to liver or other organs by hematogenous spreading before and/or after the surgical resection of PETs.

and indirectly, and promotes neoangiogenesis by recruiting endothelial progenitor cells (30). Finally, high expression of CXCL-12 in tumor cells had a close correlation with the presence of large solid nests ( $P = 0.018$ ). It is possible that CXCL-12 produced by tumor cells may mediate the formation of focal solid structures by a pair of solid growing tumor cells and their surrounding tumor-associated blood vessels with highly abnormal features. Furthermore, it is suggested that interrupting the angiogenic

pathway mediated by CXCL-12 may provide a novel and efficient antiangiogenesis strategy for the treatment of PETs.

### Acknowledgments

We thank Drs. Kazuaki Shimada, Yoshihiro Sakamoto, Hidenori Ojima, and Hiroki Ochiai for useful discussions and Kaoru Onozato, Yuko Yamauchi, Fumi Kaiya-Toshioka, Ayaka Miura, and Rie Itoh for their technical advice.

## References

1. DeLellis RA, Lloyd RV, Heitz PU, Eng C. World Health Organization classification of tumours. Pathology and genetics of tumours of endocrine organs. Lyon: IARC Press; 2004. p. 175–208.
2. Solcia E, Capella C, Klöppel G. Tumors of the pancreas. Atlas of tumor pathology. 3rd series, fascicle 20. Washington (DC): Armed Forces Institute of Pathology; 1997.
3. Maderia I, Terris B, Voss M, et al. Prognostic factors in patients with endocrine tumours of the duodeno-pancreatic area. *Gut* 1998;43:422–7.
4. Hochwald SN, Zee S, Conlon KC, et al. Prognostic factors in pancreatic endocrine neoplasms: an analysis of 136 cases with a proposal for low-grade and intermediate-grade groups. *J Clin Oncol* 2002;20:2633–42.
5. Jorda M, Ghorab Z, Fernandez G, Nassiri M, Hanly A, Nadji M. Low nuclear proliferative activity is associated with nonmetastatic islet cell tumors. *Arch Pathol Lab Med* 2003;127:196–9.
6. Deshpande V, Castillo CF, Muzikansky A, et al. Cytokeratin 19 is a powerful predictor of survival in pancreatic endocrine tumors. *Am J Surg Pathol* 2004;28:1145–53.
7. Goto A, Niki T, Terada Y, Fukushima J, Fukayama M. Prevalence of CD99 protein expression in pancreatic endocrine tumors (PETs). *Histopathology* 2004;45:384–92.
8. Hanahan D, Folkman J. Patterns and emerging mechanisms of the angiogenic switch during tumorigenesis. *Cell* 1996;86:353–64.
9. Lopez T, Hanahan D. Elevated levels of IGF-1 receptor convey invasive and metastatic capability in a mouse model of pancreatic islet tumorigenesis. *Cancer Cell* 2002;1:339–53.
10. Jain RK. Molecular regulation of vessel maturation. *Nat Med* 2003;9:685–93.
11. Morikawa S, Baluk P, Kaidoh T, et al. Abnormalities in pericytes on blood vessels and endothelial sprouts in tumors. *Am J Pathol* 2002;160:985–1000.
12. Hashizume H, Baluk P, Morikawa S, et al. Openings between defective endothelial cells explain tumor vessel leakiness. *Am J Pathol* 2000;156:1363–80.
13. Ellis LM, Fidler IJ. Tumor angiogenesis. In: Mendelsohn J, Howley PM, Israel MA, et al. editors. *The molecular basis of cancer*. 2nd ed. Philadelphia: Saunders; 2001. p. 173–85.
14. Carmeliet P, Jain RK. Angiogenesis in cancer and other diseases. *Nature* 2000;407:249–57.
15. Poon RTP, Ng IOL, Lau C, et al. Tumor microvessel density as a predictor of recurrence after resection of hepatocellular carcinoma: a prospective study. *J Clin Oncol* 2002;20:1775–85.
16. Marion-Audibert AM, Barel C, Gouysse G, et al. Low microvessel density is an unfavorable histopathologic factor in pancreatic endocrine tumors. *Gastroenterology* 2003;125:1094–104.
17. Couvelard A, O'Toole D, Turley H, et al. Microvascular density and hypoxia-inducible factor pathway in pancreatic endocrine tumours: negative correlation of microvascular density and VEGF expression with tumour progression. *Br J Cancer* 2005;92:94–101.
18. La Rosa S, Uccella S, Finzi G, Alvarello L, Sessa F, Capella C. Localization of vascular endothelial growth factor and its receptors in digestive endocrine tumors: correlation with microvessel density and clinicopathologic features. *Hum Pathol* 2003;34:18–27.
19. Tan G, Cioc AM, Perez-Montiel D, Ellison EC, Frankel WL. Microvascular density does not correlate with histopathology and outcome in neuroendocrine tumors of the pancreas. *Appl Immunohistochem Mol Morphol* 2004;12:31–5.
20. Folkman J. Clinical applications of research on angiogenesis. *N Engl J Med* 1995;333:1757–63.
21. Weidner N. Tumour vascularity as a prognostic factor in cancer patients: the evidence continues to grow. *J Pathol* 1998;184:119–22.
22. Weidner N, Semple JP, Welch WR, Folkman J. Tumor angiogenesis and metastasis - correlation in invasive breast carcinoma. *N Engl J Med* 1991;324:1–8.
23. Takahashi Y, Hiraoka N, Onozato K, et al. Solid-pseudopapillary neoplasms of the pancreas in men and women: do they differ? *Virchows Arch* 2006;448:561–9.
24. Hiraoka N, Onozato K, Kosuge T, Hirohashi S. Prevalence of FOXP3<sup>+</sup> regulatory T cells increases during the progression of pancreatic ductal adenocarcinoma and its premalignant lesions. *Clin Cancer Res* 2006;12:5423–34.
25. Eberhard A, Kahlert S, Goede V, et al. Heterogeneity of angiogenesis and blood vessel maturation in human tumours: implications for antiangiogenic tumor therapies. *Cancer Res* 2000;60:1388–93.
26. Stefansson IM, Salvesen HB, Akslen LA. Vascular proliferation is important for clinical progress of endometrial cancer. *Cancer Res* 2006;66:3303–9.
27. Grunewald M, Avraham I, Dor Y, et al. VEGF-induced adult neovascularization: recruitment, retention, and role of accessory cells. *Cell* 2006;124:175–89.
28. Bluel CC, Farzan M, Choe H, et al. The lymphocyte chemoattractant SDF-1 is a ligand for LESTR/fusin and blocks HIV-1 entry. *Nature* 1996;382:829–33.
29. Peled A, Petit I, Kollet O, et al. Dependence of human stem cell engraftment and repopulation of NOD/SCID mice on CXCR4. *Science* 1999;283:845–8.
30. Orimo A, Gupta PB, Sgroi DC, et al. Stromal fibroblasts present in invasive human breast carcinomas promote tumor growth and angiogenesis through elevated SDF-1/CXCL12 secretion. *Cell* 2005;121:335–48.